Journal of Organometallic Chemistry 693 (2008) 2649–2656

Contents lists available at ScienceDirect

Journal of Organometallic Chemistry

journal homepage: www.elsevier.com/locate/jorganchem

Synthesis, structure and characterization of *fac*-$[Re(CO)_3]^+$ complexes derived from hydrazone Schiff bases: DFT–TDDFT investigation on electronic structures

Sucharita Basak [a], Deepak Chopra [b], Kajal Krishna Rajak [a,*]

[a] Inorganic Chemistry Section, Department of Chemistry, Jadavpur University, Kolkata 700 032, India
[b] Solid State and Structural Chemistry Unit, Indian Institute of Science, Bangalore 560 012, India

ARTICLE INFO

Article history:
Received 14 February 2008
Received in revised form 16 April 2008
Accepted 22 April 2008
Available online 13 May 2008

Keywords:
Schiff base
Re(I) complex
Intermolecular interaction
DFT and TDDFT

ABSTRACT

The syntheses, structural and spectroscopic characterization of the complexes of general formula $[ReL(CO)_3Cl]$ bearing bifunctional hydrazone Schiff base ligand **L** are presented in this paper. The structure of one of the complexes is determined by X-ray crystallography. The solid-state structure of the compound is involved in a secondary interaction in lattice forming a supramolecular array. The gas phase geometry optimization and electronic calculation have been performed using density functional theory without any symmetry constraints. On the basis of structural and theoretical studies, ligand in the complexes is considered to be in the keto, not in enol form. Experimental ground state IR and NMR data set agree with those calculated by DFT calculations. The electronic spectra of the complexes are calculated by time dependent density functional theory (TDDFT) using conductor like polarizable continuum model (CPCM). The computed vertical excitation energies in solution are in good agreement with experimental one showing that the metal-to-ligand charge transfer transitions in visible region dominate over ligand based ILCT transition. The TDDFT excited states calculation of the electronic spectra in solution provides evidence towards luminescence spectra.

1. Introduction

Rhenium (I) complexes containing *fac*-$[Re(CO)_3]^+$ derived from bifunctional Schiff base ligands have aroused recent attention [1]. The compounds bearing *fac*-$[Re(CO)_3]^+$ show interesting photophysical and photochemical [1,2] properties as well as their uses in CO_2 activation [3] and in the field of supramolecular chemistry [4]. It has been documented in the literature that *fac*-$[Re(CO)_3]^+$ core also commits a convenient platform for the development of efficient radiopharmaceuticals [5,6]. Thus the interesting properties exhibited by *fac*-$[Re(CO)_3]^+$ core provides an opportunity to investigate the chemistry of Re(I) complexes incorporating bifunctional Schiff base ligands.

In this paper, we describe the synthesis of two rhenium (I) complexes of general formula $[ReL(CO)_3Cl]$ where **L** is the Schiff base of benzoyl hydrazine and pyridine-2-carboxaldehyde and 2-acetylpyridine respectively. The complexes are characterized spectroscopically. The X-ray structure of one representative case is reported. The emission spectra and electrochemical behaviors are also scrutinized.

Herein we also present the DFT calculations to investigate the geometry, electronic structure IR and NMR spectra. The absorption and emission spectra of the complexes have been examined using time dependent density functional theory (TDDFT) to establish the experimental observations.

2. Results and discussion

Two ligands $\mathbf{L}^1$ and $\mathbf{L}^2$ (abbreviated as **L**) have been used in the present work. The ligands were synthesized by condensation of benzoyl hydrazine and aldehyde or ketone. The ligand may exist both in keto and enol form in solution [7].

The stoichiometric reaction of $[Re(CO)_5Cl]$ with the synthesized ligand in boiling toluene afforded orange red color complex of general formula *fac*-$[ReL(CO)_3Cl]$ in excellent yields.

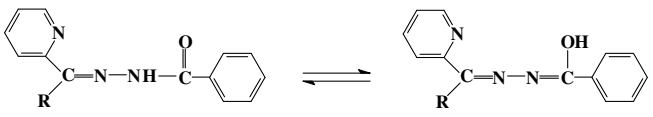

R = H ; $\mathbf{L}^1$
R = CH_3 ; $\mathbf{L}^2$

* Corresponding author.
E-mail address: kajalrajak@hotmail.com (K.K. Rajak).

0022-328X/$ - see front matter © 2008 Elsevier B.V. All rights reserved.
doi:10.1016/j.jorganchem.2008.04.047

2.1. Molecular structure of fac-[ReL^1(CO)$_3$Cl] (**1**)

The molecular structure of [ReL^1(CO)$_3$Cl] · H$_2$O has been determined by single crystal X-ray diffractometry. It crystallizes in the space group $P2_1/c$. The selected bond distances and angles are listed in Table 1 and the molecular view is shown in Fig. 1.

The coordination geometry at the Re is a distorted octahedron with three carbonyl ligands arranged in the facial fashion. The trans angles at the rhenium site fall in the range 171.0–175.0°(3) indicating a deviation from an ideal octahedral geometry. In the distorted ReN$_2$C$_3$Cl octahedral environment, two carbon atoms of the carbonyl group and two nitrogen atoms lie in the equatorial plane whereas the axial positions are occupied by chloro group and one carbonyl group. The Re–N and Re–CO bond distances are consistent with those observed in the similar complexes [8].

In the extended lattice structure a self-assembled supramolecular cluster compound is formed by simultaneous coordinative and hydrogen-bonding interaction. In the solid state, the lattice water is involved in the hydrogen bonding with coordinated chloride group and free amine nitrogen atom attached with the benzoyl group of the ligand forming a dimeric unit (Fig. 2). The O(5)···Cl(1) and O(5)···N(3) distances being 3.178(12) and 2.758(10) Å respectively. The hydrogen bonded lattice water of the dimeric unit is again hydrogen bonded with ketonic group (O(4)···O(5)), (2.733(9) Å) of the other dimeric unit and so on and this situation provides a supramolecular array.

Table 1
Selected bond lengths (Å) and angles (°) for *fac*-[Re(CO)$_3$L^{1}Cl]

Re(1)–C(1)	1.912(9)
Re(1)–C(2)	1.902(9)
Re(1)–C(3)	1.894(9)
Re(1)–N(1)	2.182(7)
Re(1)–N(2)	2.178(6)
Re(1)–Cl(1)	2.486(2)
C(2)–Re(1)–C(3)	90.8(4)
C(2)–Re(1)–C(1)	88.2(4)
C(3)–Re(1)–C(1)	87.1(4)
C(2)–Re(1)–N(1)	93.1(3)
C(3)–Re(1)–N(1)	98.0(3)
C(1)–Re(1)–N(1)	174.7(3)
C(3)–Re(1)–N(2)	171.0(3)
C(2)–Re(1)–N(2)	93.7(3)
C(1)–Re(1)–N(2)	100.9(3)
N(1)–Re(1)–N(2)	74.0(2)
C(2)–Re(1)–Cl(1)	175.0(3)
C(3)–Re(1)–Cl(1)	94.2(3)
C(1)–Re(1)–Cl(1)	92.8(3)
N(1)–Re(1)–Cl(1)	85.50(18)
N(2)–Re(1)–Cl(1)	81.28(17)

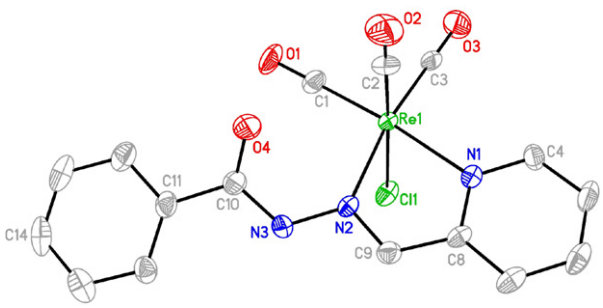

Fig. 1. Perspective view and atom-labeling scheme for molecule [ReL^1(CO)$_3$Cl]. All non-hydrogen atoms are represented by their 30% thermal probability ellipsoids.

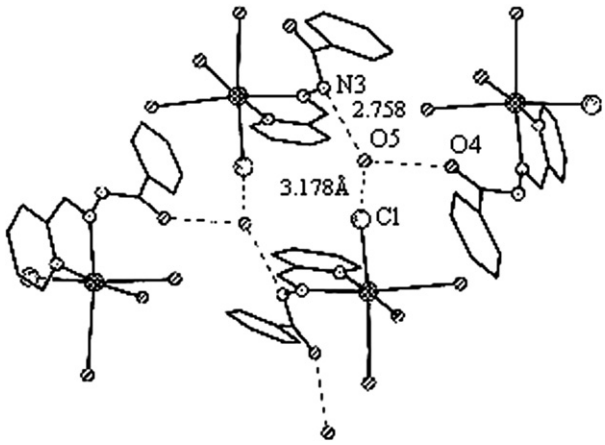

Fig. 2. Intermolecular interaction: dimeric unit; hydrogen atoms not participating in the interaction are excluded for clarity.

2.2. Geometry and electronic structure

The complexes are diamagnetic at room temperature indicating their singlet ground state (t_{2g}^6). The geometry optimization of complexes **1** and **2** was performed in gas phase in their singlet spin state. The geometry used for the ground state optimization is based on crystal structure parameter for complex **1**, but we are unable to grow the single crystal suitable for X-ray structure determination in case of complex **2**. Therefore the significant bond distances and angles of the optimized geometry of both the complexes in gas phase are compared with the crystal structure parameter of **1** and are given in Table 2. The gas phase optimized structure of complex **2** is represented in Fig. 3 and it is very much comparable with the optimized structure of complex **1** (Supporting information, Fig. S1). The crystal structure data of **1** (Table 1) is in excellent

Table 2
Calculated bond distance (Å) and selected bond angles (°) for complex **1** and **2**

	Gas phase	
	Complex **1**	Complex **2**
Re(1)–C(1)	1.9240	1.9273
Re(1)–C(2)	1.9155	1.9116
Re(1)–C(3)	1.9275	1.9299
Re(1)–N(1)	2.1883	2.1818
Re(1)–N(2)	2.1985	2.1709
Re(1)–Cl(1)	2.5376	2.5464
N(1)–Re(1)–N(2)	74.81	73.65
N(1)–Re(1)–Cl(1)	84.33	83.94
N(2)–Re(1)–Cl(1)	84.48	82.72

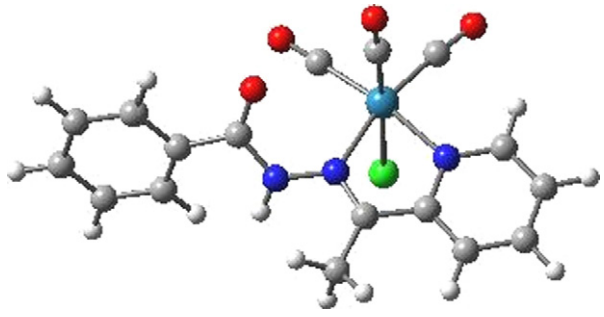

Fig. 3. Optimized molecular structure of [ReL^2(CO)$_3$Cl]. (Re: Cyan, Cl: Green, N: Blue, O: Red, C: Grey, H: White). (For interpretation of the references to colour in this figure legend, the reader is referred to the web version of this article.)

agreement with optimized parameters (maximum deviation 0.05 Å for Re–Cl bond distance and 0.02 Å for all other bond distances). The optimized geometries of the two complexes do not show significant differences in the coordinate sphere around the metal center. It reveals that the ligands bind in a similar fashion in the complexes.

A schematic molecular orbital energy level diagram for 12 frontier orbitals of complexes **1** and **2** is shown in Fig. 4. The isodensity plot from HOMO−5 to LUMO+5 for **1** is shown in Fig. 5 (Same plot for complex **2** is given in supporting information, Fig. S2). The detailed contributions from different fragment to the frontier orbital for both the complexes are given in Table 3.

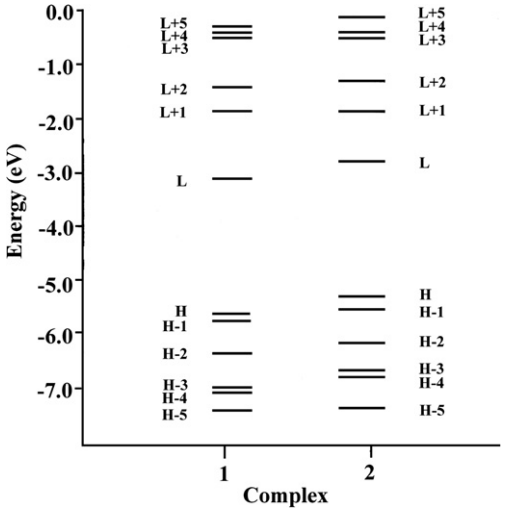

Fig. 4. Schematic molecular orbital energy diagram for six occupied (H) and six virtual (L) frontier orbitals of the complexes in the singlet ground state (H = HOMO, L = LUMO).

In both cases the HOMO and HOMO−1 are lying within 0.175 eV. The HOMO and HOMO−1 of the complexes contained ~45% or more Rhenium d orbital contribution, 30% or more chlorine orbital and ~15% or more CO_x contribution. HOMO−1 can be described as the in-phase combination of π^* orbital of carbonyls with metal d orbital and out-phase with chlorine, while HOMO−2 is lying 0.664 eV below the HOMO having ~65% metal d orbital contribution and ~25% π^* orbital of the carbonyls. The HOMO−3 and HOMO−4 are almost degenerate (energy difference 0.052 eV) and the HOMO−3, HOMO−4 and HOMO−5 are lying 1.391, 1.443 and 1.657 eV below that of HOMO, respectively, predominantly contribution arises from chlorine, CO_x and ligand part. The LUMO, LUMO+1 and LUMO+2 for both the complexes were found to be largely of the Schiff base ligand contribution. LUMO+3 and LUMO+5 for **1** while LUMO+4 and LUMO+5 for **2** are having about 50% contribution from carbonyls and 20% of metal orbital contribution. In complex **1** LUMO+4 and in **2** LUMO+3, the electron density was localized on the benzene ring bearing benzoyl group.

The ground state energy of the complexes was also calculated in acetonitrile solution using CPCM model. In acetonitrile solution the calculated energy of the complexes **1** and **2** are lowered by a value 1.184 eV and 1.605 eV, respectively, but the composition of the frontier orbitals remains unchanged.

2.3. IR spectra

The complexes display three metal carbonyl vibrations in the region 1880–2030 cm^{-1}. These vibrations are consistent with the

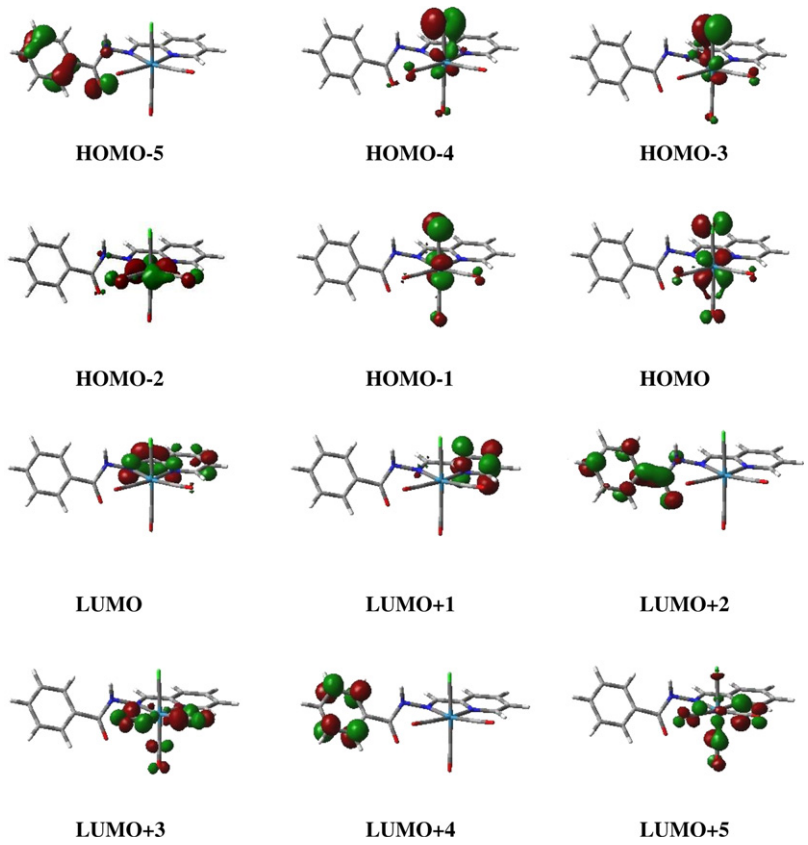

Fig. 5. Isodensity plot of the frontier orbitals of $[ReL^1(CO)_3Cl]$.

Table 3
Energies (eV) and composition (%) of frontier molecular orbitals of the complex **1** and **2**

Orbital	*E* (eV)	Re	–Cl	∑CO	Ligand
1					
HOMO−5	−7.300	2.7	2.1	2.6	92.6
HOMO−4	−7.086	20.2	59.5	8.6	11.7
HOMO−3	−7.034	20.3	53.9	9.3	16.5
HOMO−2	−6.307	63.4	1.0	24.8	10.8
HOMO−1	−5.818	38.0	37.6	14.9	9.5
HOMO	−5.643	44.2	30.9	19.2	5.7
LUMO	−3.142	8.6	3.4	7.7	80.3
LUMO+1	−1.863	1.5	0.4	2.2	95.9
LUMO+2	−1.479	1.4	0.1	1.3	97.2
LUMO+3	−0.527	19.7	2.4	53.3	24.6
LUMO+4	−0.405	1.7	0.5	2.7	95.1
LUMO+5	−0.364	20.0	10.3	50.1	19.6
2					
HOMO−5	−7.287	2.6	3.7	3.3	90.4
HOMO−4	−6.818	21.8	57.3	9.8	11.1
HOMO−3	−6.772	18.3	48.4	8.3	25.0
HOMO−2	−6.112	63.1	1.4	25.0	10.5
HOMO−1	−5.609	37.3	38.9	15.0	8.8
HOMO	−5.417	44.1	31.4	19.0	5.5
LUMO	−2.897	7.3	2.9	6.6	83.1
LUMO+1	−1.721	2.1	0.5	2.5	94.9
LUMO+2	−1.311	1.1	0.1	1.2	97.6
LUMO+3	−0.511	0.7	0.1	0.8	98.4
LUMO+4	−0.310	18.0	3.0	44.9	34.1
LUMO+5	−0.136	20.9	9.9	55.7	13.5

presence of *fac*-$[Re(CO)_3]^+$ core in the complex with approximate pseudo C_{3V} symmetry. The C═N stretch are observed at 1605 and 1559 cm^{-1} while that of Re–Cl at 302 and 305 cm^{-1} for **1** and **2**, respectively. The bands occur about 1680 and 3420 cm^{-1} is due to C═O and N–H of the ligand. The frequencies calculated by DFT method using the gas phase optimized structure predict three carbonyl vibrations with a_1 and e symmetries [9]. The calculation also reveals the presence of C═N and C═O vibrations in the complexes. It is documented that the DFT calculations underestimate the vibration energies in some cases [10] and in the present case the absolute value of calculated frequencies are lower than the experimental values. The experimental and calculated characterization data are given in Section 3.

2.4. NMR spectra

The complexes are diamagnetic and display well resolved ^1H and ^{13}C NMR spectra in solution. The assignment of NMR spectra was based on intensity and spin–spin splitting structure of the Re(I) complexes. A representative ^1H NMR spectrum of **1** is shown in Fig. 6a.

Both the complexes display a sharp peak near 9.5 ppm due to N–*H* proton, which disappears upon shaking with D_2O. The C(4)–*H* proton observed as doublet at ∼9.0 ppm. The singlet near 10.2 ppm for **1** corresponds to the azomethine hydrogen atom. The aromatic proton chemical shifts are observed within the range ∼7.0–9.0 ppm. The resonance of $-CH_3$ group for **2** is observed at ∼3.47 ppm.

The complexes show three metal carbonyl resonances in the region 188–199 ppm describing the presence of pseudo-C_3 *fac*-$[Re(CO)_3]^+$ [8] core. The closely spaced resonances (197.5 and 198.7 ppm) are assigned as equatorial carbonyls whereas resonance at 188.9 ppm is ascribed to the axial carbonyl group. The observed differences between the chemical shift in the equatorial and axial carbonyl groups can be attributed to stronger π-acceptor property of the nitrogen atom of the Schiff base ligand than that of chloro group.

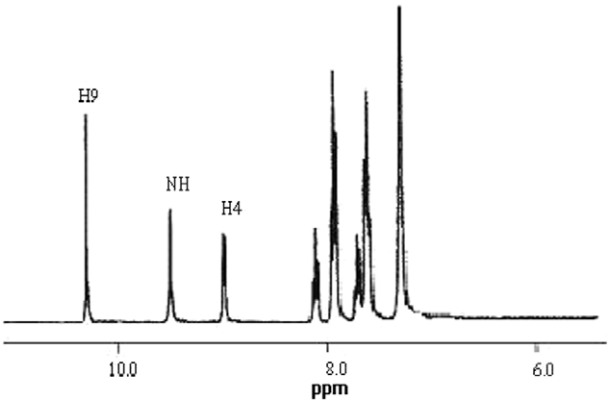

Fig. 6a. ^1H NMR spectrum of $[ReL^1(CO)_3Cl]$ in CD_3CN at room temperature.

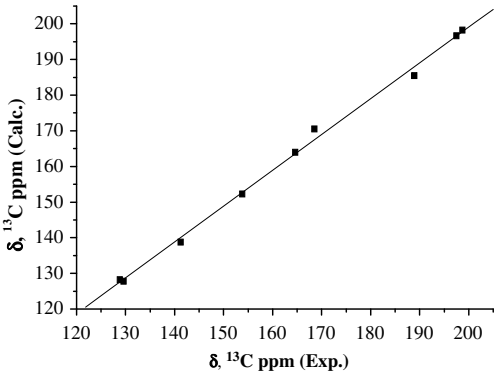

Fig. 6b. Linear correlation between the experimental and calculated ^{13}C NMR chemical shifts of $[ReL^1(CO)_3Cl]$.

In the present case, the calculated NMR spectral chemical shifts agree well with the experimental data. The experimental and calculated NMR data are given in Section 3. The correlation between the experimental and calculated ^{13}C NMR chemical shift of complex **1** is shown in Fig. 6b.

2.5. Electrochemical studies

It has been reported earlier [11] that the study of electrochemical behavior is an important phenomenon of the complexes involving HOMO and LUMO in the redox processes. In the present case, the complexes are electroactive in acetonitrile solution at Platinum electrode vs SCE. The cyclic voltammogram was recorded at a scan rate of 50 mV/s. The relevant data are given in Section 3 and a representative voltammogram is shown in supporting information (Fig. S3). In both the complexes HOMO consist of 45% metal d, 30% of chloro and 15% $(CO)_x$ character while the LUMO is mainly localized on Schiff base ligands. Thus the oxidation (∼1.20 V) i.e. the removal of electron from orbital containing a metal $d\pi$ character with a considerable contribution from Cl and $(CO)_x$ is probably responsible for irreversible electrochemical behavior. On the other hand, the one electron reduction (∼−1.10 V) involved addition of one electron to the π^* orbital of the ligand moiety.

2.6. Absorption spectra

The absorption spectra of the complexes were examined in acetonitrile solution at room temperature. The electronic spectral data are given in Section 3.

The visible absorption spectra of the complexes appear as a broad absorption band at 400 nm. The band is attributed to MLCT

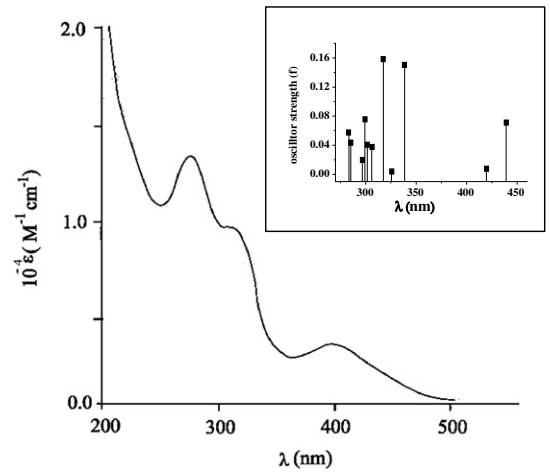

Fig. 7. Experimental absorption spectrum of $[ReL^1(CO)_3Cl]$ in acetonitrile solution. Inset: Calculated absorption spectra of $[ReL^1(CO)_3Cl]$. The excited states are shown as vertical bars with height equal to the oscillator strength.

[2b,12,13a,13c] [Re($d\pi$) → L($\pi-$)] transition. The shoulder at about 310 nm is due to mixed MLCT and ILCT excitations. The intense absorption band at higher energy (~290 nm) is presumably due to intra ligand transition from $\pi \rightarrow \pi^*$ excitation that is localized on the conjugate ligand.

A comparison of calculated (vertical excitations) and experimental spectra for complex **1** is reported in Fig. 7. The most representative optical transition for **1** are listed in Table 4. (for **2**, see supporting information, Table S1). The detailed discussion for **1** has been made. The bands/shoulders appeared in the calculated spectra are about 0.2 eV red shifted compared to the experimental spectra. In the calculated spectra, the band centered about 400 nm, appears to be a composition of two excitations at 2.82 eV (λ = 439.2 nm, f = 0.0711) and 2.95 eV (λ = 419.8 nm, f = 0.0076) and is due to HOMO−1 to LUMO, HOMO−2 to LUMO and HOMO−3 to LUMO transition, respectively. Thus the transition at ~400 nm, is logically be assigned as MLCT transition. The main orbital contribution to the transition at ~310 nm which appears as shoulder, arises from the HOMO−3 to LUMO, HOMO−4 to LUMO, HOMO−5 to LUMO, HOMO to LUMO+1 and the HOMO−1 to LUMO+1. This transition can be described as a superposition of the transitions at 3.66 eV (λ = 338.4 nm, f = 0.1504), 3.90 eV (λ = 317.3 nm, f = 0.1582) and at 4.05 eV (λ = 306.4 nm, f = 0.0376). Therefore this transition has a mixed ILCT and MLCT charge transfer character. The more intense absorption at higher energy ($\lambda \sim 290$ nm) also consists of more than one excitation. The excitations observed at energies respectively 4.11 eV (λ = 301.5 nm, f = 0.0406), 4.14 eV (λ = 299.3 nm, f = 0.0755), 4.17 eV (λ = 296.7 nm, f = 0.0198), 4.34 eV (λ = 285.2 nm, f = 0.0434) and 4.38 eV (λ = 283.1 nm, f = 0.0574).

2.7. Emission spectra and triplet excited state for *1*

Photoluminescence spectra for the complex **1** in acetonitrile was recorded after excitation at λ = 390 nm. The complex was luminescent [2d,13] at room temperature with a broad emission band centered on 465 nm. The experimental emission spectrum of **1** is shown in Fig. 8.

The photoluminescence properties mainly originating from triplet state charge transfer transition. Thus the lowest lying triplet state geometry of the complex was optimized using unrestricted B3LYP method in the gas phase. The $\langle S^2 \rangle$ value is 2.0080, indicating minimal spin contamination from the state of higher spin multiplicity. The energy of lowest spin state of the complexes is higher by 11 332 cm^{-1} from its ground state. The lowest lying triplet state is of MLLCT origin and this is a characteristic feature of the single occupancy of HOMO and LUMO. The emission band determined in the calculated spectra is about 0.15 eV red shifted compared to the experimental spectra. The calculation suggests that the transition centered at 482 nm is a combination of three excitation and MLLCT in nature; mainly originating as the transition from HOMO to LUMO along with HOMO−4 to LUMO and HOMO−5 to LUMO,

Table 4
Main calculated optical transition with composition in terms of molecular orbital contribution of the transition, vertical excitation energies and oscillator strength in acetonitrile

Excitation	Composition	E (eV)	Oscillator strength (f)	λ_{theo} (nm)	λ_{exp} (nm)
1	HOMO−1 → LUMO (95%)	2.82	0.0711	439.2	398
2	HOMO−3 → LUMO (87%) HOMO−2 → LUMO (10%)	2.95	0.0076	419.8	
3	HOMO−4 → LUMO (19%) HOMO−3 → LUMO (73%) HOMO → LUMO+1 (6%)	3.66	0.1504	338.0	310
4	HOMO−4 → LUMO (46%) HOMO−3 → LUMO (10%) HOMO−1 → LUMO+1 (9%) HOMO → LUMO+1 (32%)	3.90	0.1582	317.2	
5	HOMO−5 → LUMO (52%) HOMO−4 → LUMO (16%) HOMO−1 → LUMO+1 (21%) HOMO → LUMO+1 (10%)	4.05	.0376	306.4	
6	HOMO−5 → LUMO (21%) HOMO−1 → LUMO+1 (62%)	4.11	0.0406	301.5	290
7	HOMO−6 → LUMO (58%) HOMO−3 → LUMO+1 (10%) HOMO−1 → LUMO+1 (14%)	4.14	0.0755	299.3	
8	HOMO−6 → LUMO (20%) HOMO−7 → LUMO (65%)	4.17	0.0198	296.7	
9	HOMO−2 → LUMO+1 (42%) HOMO → LUMO+3 (16%) HOMO → LUMO+4 (10%)	4.34	0.0434	285.2	
10	HOMO−8 → LUMO (13%) HOMO−2 → LUMO+1 (7%) HOMO−2 → LUMO+3 (20%) HOMO → LUMO+3 (17%) HOMO → LUMO+4 (8%)	4.38	0.0574	283.1	

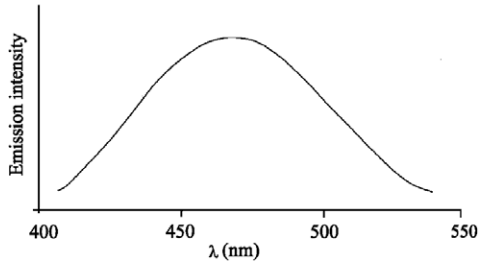

Fig. 8. The luminescence spectra of $[ReL^1(CO)_3Cl]$ in acetonitrile solution (excitation wavelength: 390 nm).

where the HOMO contains ~45% Re d character and HOMO−4 and HOMO−5 are mainly having ligand orbital contribution. The calculated value is comparable with experimental result (Table 5).

2.8. Conclusion

In summary, we synthesized and characterized the *fac*-$[Re(CO)_3]^+$ complexes incorporating bifunctional hydrazone ligands. The uncoordinated ketonic function plays a crucial role towards the formation of supramolecular arrangement in the lattice. We have performed a comprehensive study of the electronic structure of the complexes. The optimized geometries, frequencies, energies, frontier orbitals and excited states that emerged from the calculations provided a detailed description of the IR, NMR, absorption and emission properties of the complexes. Study on different Re(I) species using various O, N coordinating ligands along with their theoretical investigations are in progress.

3. Experimental

3.1. Materials

$[Re(CO)_5Cl]$ (98%) was used as purchased from Aldrich Chemical Co. All of the chemicals and solvents were analytically pure and used without further purification.

Table 5
Calculated triplet excited states of complex **1** in acetonitrile based on the lowest lying triplet state geometry. Main calculated vertical transition with composition in terms of molecular orbital contribution of the transition, Vertical excitation energies and oscillator strength

State	Excitation	Energy (eV)	Oscillator strength (f)	Λ (nm) (calc.)	Λ (nm) (exp.)
1	HOMO → LUMO (100%)	2.4267	0.0022	510.9	465
2	HOMO → LUMO (58%) HOMO−1 → LUMO (13%) HOMO−4 → LUMO (14%) HOMO−5 → LUMO (15%)	2.5183	0.0000	492.3	
3	HOMO → LUMO (7%) HOMO−1 → LUMO (14%) HOMO−2 → LUMO (30%) HOMO−3 → LUMO (8%) HOMO−4 → LUMO (19%) HOMO−5 → LUMO (21%)	2.7967	0.0000	443.3	

3.2. Physical measurements

UV–Vis spectra were recorded on a Perkin–Elmer LAMBDA 25 spectrophotometer. IR spectra were obtained with a Perkin–Elmer L-0100 spectrophotometer. ^1H and ^{13}C NMR spectra were measured on Bruker FT 300 MHz spectrometer and Bruker FT 500 MHz spectrometer, respectively. The atom-numbering scheme used for ^1H and ^{13}C is same as that used in the crystallography. Elemental analyses were performed on Perkin–Elmer 2400 series II analyzer and electrochemical measurements were recorded on a CHI 620A electrochemical analyzer using platinum electrode under a dinitrogen atmosphere. Tetra ethyl ammonium perchlorate (TEAP) was used as a supporting electrolyte and potentials are referenced to the Standard Calomel Electrode (SCE) without junction correction. The Emission data were collected on a Hitachi F4 500 fluorescence spectrophotometer.

3.3. X-ray structure determination

The single crystal suitable for X-ray crystallographic analysis of the complex $[ReL^1(CO)_3Cl] \cdot H_2O$ was obtained by diffusing dichloromethane solution of the complex into the hexane. The X-ray intensity data were collected on Bruker AXS SMART APEX CCD diffractometer (Mo Kα, $\lambda = 0.71073$ Å) at 293 K. The detector was placed at a distance 6.03 cm from the crystal. Total 606 frames were collected with a scan width of 0.3° in different settings of φ. The data were reduced in SAINTPLUS [14] and empirical absorption correction was applied using the SADABS package [14]. Metal atom was located by Patterson Method and the rest of the non-hydrogen atoms were emerged from successive Fourier synthesis. The structures were refined by full matrix least-square procedure on F^2. All non-hydrogen atoms were refined anisotropically. All Calculations were performed using the SHELXTL V 6.14 program package [15]. Molecular structure plots were drawn using ORTEP [16]. Relevant crystal data are given in Table 6.

3.4. Computational details

All the calculations were carried out with the density functional theory (DFT) [17] method and the calculations have been performed using the B3LYP exchange correlation functional [18], as implemented in GAUSSIAN 03 (G03) program package [19]. The geometry of the complexes **1** and **2** were fully optimized in gas

Table 6
Crystal data and structure refinement parameters for complex $[Re(CO)_3L^1Cl] \cdot H_2O$

1	
Formula	$C_{16}H_{11}ClN_3O_5Re$
Formula weight	548.94
Crystal system	Monoclinic
Space group	$P2_1/c$
a (Å)	8.602(3)
b (Å)	15.484(6)
c (Å)	13.638(5)
α (°)	90.000
β (°)	90.987(6)
γ (°)	90.000
V (Å^3)	1816.2(12)
Z	4
D_{calc} (mg m^{-3})	2.008
μ, Mo Kα (mm^{-1})	6.870
θ (°)	1.99–25.00
Measured reflection	12 551
Unique reflection (R_{int})	3199 (0.0723)
Temperature (K)	293(2)
R_1,[a] wR_2[b] [$I > 2\sigma(I)$]	0.0454, 0.1025
GOF on F^2	1.040

[a] $R_1 = \sum |F_o| - |F_c| / \sum |F_o|$.
[b] $wR_2 = [\sum w(F_o^2 - F_c^2)^2 / \sum w(F_o^2)^2]^{1/2}$.

phase using 6-31G* basis set [20] for H, C, N, O, Cl atoms and Lanl2dz [21] basis set along with the corresponding pseudo potential [21c] for rhenium without any symmetry constrain. The vibrational frequency calculation was also performed for both the complexes to ensure that the optimized geometries represent the local minima and there are only positive eigen values. The single crystal X-ray coordinates has been used in all calculations for **1**; and for **2**, the gas phase optimized structure was used. There is a good agreement between the theoretical and experimental structures. The NMR spectra of the complexes ware carried out using GIAO [22] method incorporated in GAUSSIAN 03W. To assign the low lying electronic transitions in the experimental spectra, TDDFT [23] calculations of the complexes were done in acetonitrile using conductor-like polarizable continuum model (CPCM) [24] with larger basis set 6-31g+(d) for H, C, N, O, Cl and Lanl2dz for rhenium. We computed the lowest 20 singlet – singlet transition and results of the TD calculations was qualitatively very similar. VMOdes A 7.1 [25] program was used to calculate the molecular orbital contributions from groups or atoms.

3.5. Synthesis of the complexes

The complexes $[ReL(CO)_3Cl]$ were prepared by using a general method with $[Re(CO)_5Cl]$. Details are given below for one representative case.

3.6. $[ReL^1(CO)_3Cl]$ (**1**)

L^1 (63 mg, 0.27 mmol) and $Re(CO)_5Cl$ (100 mg, 0.27 mmol) were refluxed in 15 ml of toluene for 6 h. After cooling to room temperature, the solvent was removed under reduced pressure. The crude mass was dissolved in a minimum volume of dichloromethane and subjected to a column chromatography on a silica gel column (12×1 cm, 60–120 mesh). A red orange band was eluted using benzene–acetonitrile (5:1) mixture. A red-orange colored solid was obtained after removal of solvent under reduced pressure. The product was recrystallized from dichloromethane–hexane. 85 mg (60% yield). Anal. Calc. for $C_{16}H_{11}ClN_3O_4Re$ (530.5): C, 36.22; H, 2.07; N, 7.92. Found: C, 36.87; H, 2.11; N, 8.01%. IR_{exp} (KBr): ν(Facial 3CO) 2023, 1907 and 1890, ν(C=N) 1605, ν(C=O) 1695, ν(Re–Cl) 302, ν(N–H) 3422 cm^{-1}. IR_{theo} (KBr): ν(Facial 3CO) 1894, 1874 and 1979, ν(C=N) 1596, ν(C=O) 1669, ν(Re–Cl) 281, ν(N–H) 3664 cm^{-1}. UV/Vis [CH_3CN]: λ_{max} (ε, M^{-1} cm^{-1}) = 398 nm (3723), 310 nm (9574), 290 nm (13830). ^1H NMR_{exp} (CD_3CN): δ 10.2 (H9, s), 9.5 (N*H*, s), 8.9 (H4, d, J = 5.5), 8.1 (H6, t, J = 7.0), 7.9 (H7, t, J = 7.3), 7.6 (H5, m), 7.0–9.0 (aromatic *H*'s). ^1H $NMR_{theor.}$: δ 10.4 (H9), 9.0 (N*H*, s), 8.8 (H4), 7.7 (H6), 7.6 (H7), 7.5 (H5), 6.0–8.0 (aromatic *H*'s). ^{13}C NMR_{exp} (CD_3CN): δ 198.7, 197.5, 188.9 (3*C*O's), 168.5 (C10), 164.6 (C9), 154.2 (C8), 153.8 (C4), 141.2 (C6), 129.6 (C7), 128.8 (C5), 127.0–140.0 (aromatic *C*'s). ^{13}C NMR_{theor}: δ 198.2, 196.7, 185.5 (3*C*O's), 170.5 (C10), 164.0 (C9), 156.2 (C8), 152.3 (C4), 138.8 (C6), 128.2 (C5), 127.8 (C7), 100.0–140.0 (aromatic *C*'s). E_{pa} (Re^I/Re^{II} couple): 1.30 V (irr); E_{pc} (ligand reduction couple): −1.10 V (irr.).

3.6.1. $[ReL^2(CO)_3Cl]$ (**2**)

82 mg (55% yield) Anal. Calc. for $C_{17}H_{13}ClN_3O_4Re$ (544.5): C, 37.50; H, 2.38; N, 7.72. Found: C, 36.97; H, 2.05; N, 7.38%. IR_{exp} (KBr): ν(Facial 3CO) 2027, 1902 and 1885, ν(C=N) 1559, ν(C=O) 1690, ν(N–H) 3418, ν(Re–Cl) 305 cm^{-1}. IR_{theo} (KBr): ν(Facial 3CO) 1878, 1894 and 1977, ν(C=N) 1599, ν(C=O) 1664, ν(N–H) 3620, ν(Re–Cl) 272 cm^{-1}. UV/Vis [CH_3CN]: λ_{max} (ε, M^{-1} cm^{-1}) = 400 nm (3804), 302 nm (10870), 285 nm (14130). ^1H NMR_{exp} (CD_3CN): δ 9.3 (N*H*, s), 9.1 (H4, d, J = 5.3), 7.9 (H7, t, J = 7.4), 7.8 (H6, t, J = 7.1), 7.5 (H5, m), 7.0–9.0 (aromatic *H*'s), 3.4 (CH_3, s). $NMR_{theor.}$: δ 8.7 (N*H*), 8.1 (H4), 7.2 (H6), 7.0 (H7), 6.8 (H5), 6.5–7.8 (aromatic *H*'s), 2.4 (CH_3). ^{13}C NMR_{exp}: δ 196.3, 194.8, 189.8 (3*C*O's), 165.3 (C10), 161.4 (C9), 153.9 (C8), 152.5 (C4), 138.7 (C6), 129.1 (C7), 124.2 (C5), 124.0–140.0 (aromatic *C*'s), 20.2 (-*C*H_3). ^{13}C NMR_{theo}: δ 202.1, 199.6, 192.8 (3*C*O's), 163.2 (C10), 159.8 (C9), 147.50 (C8), 142.5 (C4), 132.6 (C6), 125.70 (C7), 120.9 (C5), 124.0–140.0 (aromatic *C*'s), 16.5 (-*C*H_3). E_{pa} (Re^I/Re^{II} couple): 1.10 V (irr); E_{pc} (ligand reduction couple): −1.20 V (irr).

Acknowledgements

Financial supports from The University Grant Commission, New Delhi, India, and Department of Science and Technology, New Delhi, Council of Scientific and Industrial Research, New Delhi India is greatly acknowledged. We are also thankful to DST for the data collection on the CCD facility setup (Indian Institute of Science, Bangalore, India) under IRHPA-DST program.

Appendix A. Supplementary material

CCDC 648355 contain the supplementary crystallographic data for this paper. These data can be obtained free of charge from The Cambridge Crystallographic Data Centre via www.ccdc.cam.ac.uk/data_request/cif. Supplementary data associated with this article can be found, in the online version, at doi:10.1016/j.jorganchem.2008.04.047.

References

[1] (a) R.S. Herrick, I. Wrona, N. McMicken, G. Jones, C.J. Ziegler, J. Shaw, J. Organomet. Chem. 689 (2004) 4848;
(b) J.M. Villegas, S.R. Stoyonov, W. Huang, D.P. Rillema, J. Chem. Soc., Dalton Trans. (2005) 1042.
[2] (a) I.R. Farrell, A. Vlcek Jr., Coord. Chem. Rev. 208 (2000) 87;
(b) D.R. Striplin, G.A. Crosby, Coord. Chem. Rev. 211 (2001) 163;
(c) K. Wang, L. Huang, L. Gao, L. Jin, C. Huang, Inorg. Chem. 41 (2002) 3353;
(d) O.S. wenger, L.M. Henling, M.W. Day, J.R. Winkler, H.B. Gray, Inorg. Chem. 43 (2004) 2043;
(e) P.J. Walsh, K.C. Gordon, N.J. Lundin, A.G. Blackman, J. Phys. Chem. A 109 (2005) 5933;
(f) A.S. Polo, M.K. Itokatu, K.M. Frin, A.O.T. Patrocinio, N.Y. Murakami Iha, Coord. Chem. Rev. 250 (2006) 1669;
(g) A. Vlcek Jr., M. Busby, Coord. Chem. Rev. 250 (2006) 1755.
[3] (a) J.P. Collin, J.P. Sauvage, Coord. Chem. Rev. 93 (1989) 245;
(b) P. Christensen, A. Hamnett, A.V.G. Muir, J.A. Timney, J. Chem. Soc., Dalton Trans. (1992) 1455;
(c) G.J. Stor, F. Hartl, J.W. Van outerstep, D.J. Stufkens, Organometallics 14 (1995) 1115;
(d) F.P.A. Johnson, M.W. George, F. Hartl, J.J. Turner, Organometallics 15 (1996) 3374;
(e) T. Scheiring, A. Klein, W.J. Kaim, J. Chem. Soc., Perkin Trans. 2 (1997) 2569;
(f) B.R. Rossenaar, F. Hartl, D.J. Stufkens, Inorg. Chem. 35 (1996) 6194.
[4] (a) R.V. Slone, D.I. Yoon, R.M. Calhoun, J.T. Hupp, J. Am. Chem. Soc. 117 (1995) 11813;
(b) V. Balzani, A. Juris, M. Venturi, S. Campagna, S. Serroni, Chem. Rev. 96 (1996) 759;
(c) R.V. Slone, J.T. Hupp, Inorg. Chem. 36 (1997) 5422.
[5] (a) R. Alberto, R. Schibli, D. Angst, P.A. Schubiger, U. Abram, S. Abram, T.L.A. Kaden, Transition Met. Chem. 22 (1997) 597;
(b) R. Alberto, R. Schibli, D. Angst, A. Egli, P.A. Schubiger, J. Am. Chem. Soc. 120 (1998) 7987;
(c) R. Alberto, R. Schibli, D. Angst, P.A. Schubiger, J. Am. Chem. Soc. 121 (1999) 6076;
(d) R. Waibei, R. Alberto, J. Finnern, R. Schibli, A. Stichelberger, A. Egli, U. Abram, J.P. Mach, A. Pluckthun, P.A. Schubiger, Nat. Biotechnol. 17 (1999) 897.
[6] (a) R. Schibli, R. LaBella, R. Alberto, L. Garcia-Garayoa, K. Ortner, U. Abram, P.A. Schubiger, Bioconjugate Chem. 11 (2000) 345;
(b) A. Amann, C. Decristoforo, I. Ott, M. Wenger, D. Bader, R. Alberto, G. Putz, Nucl. Med. Biol. 28 (2001) 243;
(c) J. Wald, R. Alberto, K. Ortner, L. Candreia, Angew. Chem., Int. Ed. 40 (2001) 3062;
(d) R. Petrig, R. Schibli, C. Dumas, R. Alberto, P.A. Schubiger, Chem. Eur. J. 7 (2001) 1868.
[7] S.P. Rath, K.K. Rajak, S. Mondal, A. Chakrovorty, J. Chem. Soc., Dalton Trans. (1998) 2097.
[8] (a) K. Tani, H. Sakurai, H. Fujii, T. Hirao, J. Organomet. Chem. 689 (2004) 1665;
(b) M. Lipowska, R. Cini, G. Tamasi, X. Xu, A.T. Taylor, L.G. Marzilli, Inorg.

Chem. 43 (2004) 7774;
(c) M. Busby, A. Gabrielsson, P. Matousek, M. Towrie, A.J. Dibilio, H.B. Gray, A. Vlcek Jr., Inorg. Chem. 43 (2004) 4994;
(d) N. Lazarova, J. Babich, J. Valliant, P. Schaffer, S. James, J. Zubeita, Inorg. Chem. 44 (2005) 6763;
(e) G. Wu, D.R. Glass, D. May, W.H. Watson, D. Weidenfeld, M.G. Richmond, J. Organomet. Chem. 690 (2005) 4993.
[9] R.W. Balk, D.J. Stufkens, A. Oskam, J. Chem. Soc., Dalton Trans. (1981) 1124.
[10] (a) J.B. Forseman, A.E. Frisch, Exploring Chemistry with Electronic Structure Methods, 2nd ed., Gaussian Inc., Pittsburgh, PA, 1996;
(b) V.N. Nemykin, J.G. Olsen, E. Perera, P. Basu, Inorg. Chem. 45 (2006) 3557.
[11] L. Wallace, D.P. Rillema, Inorg. Chem. 32 (1993) 3936.
[12] (a) S.M. Fredericks, J.C. Luong, M.S. Wrighton, J. Am. Chem. Soc. 101 (1979) 7415;
(b) B.D. Rossener, D.J. Stufkens, A. Vlcek Jr., Inorg. Chem. 35 (1996) 2902.
[13] (a) M.S. Wrighton, D.L. Morse, J. Am. Chem. Soc. 96 (1974) 998;
(b) W.K. Smoothers, M.S. Wrighton, J. Am. Chem. Soc. 105 (1983) 1067;
(c) L.A. Worl, R. Duesing, P. Chen, L.D. Ciana, T.J. Meyar, J. Chem. Soc., Dalton Trans. (1991) 849;
(d) D.M. Dattelbaum, R.L. Martin, J.R. Schoonver, T.J. Meyar, J. Phys. Chem. A 108 (2004) 3518;
(e) K.K.-W. Lo, K.H.-K. Tsang, Organometallics 23 (2004) 3062.
[14] Bruker, SMART, SAINT, SADABS, XPREP, SHELXTL, Bruker AXS Inc. Madison, WI, USA, 1998.
[15] G.M. Sheldrick, SHELXTL version.6.14, Bruker AXS Inc. Madison, WI, 2003.
[16] C.K. Johnson, ORTEP, Report ORNL-5138, Oak Ridge National Laboratory, Oak Ridge, TN, 1976.
[17] R.G. Parr, W. Yang, Density-functional Theory of Atoms and Molecules, Oxford University Press, Oxford, UK, 1989.
[18] A.D. Becke, J. Chem. Phys. 98 (1993) 5648.
[19] M.J. Frisch, G.W. Trucks, H.B. Schlegel, G.E. Scuseria, M.A. Robb, J.R. Cheeseman, J.A. Montgomery, Jr., T. Vreven, K.N. Kudin, J.C. Burant, J.M. Millam, S.S. Iyengar, J. Tomasi, V. Barone, B. Mennucci, M. Cossi, G. Scalmani, N. Rega, G.A. Petersson, H. Nakatsuji, M. Hada, M. Ehara, K. Toyota, R. Fukuda, J. Hasegawa, M. Ishida, T. Nakajima, Y. Honda, O. Kitao, H. Nakai, M. Klene, X. Li, J.E. Knox, H.P. Hratchian, J.B. Cross, V. Bakken, C. Adamo, J. Jaramillo, R. Gomperts, R.E. Stratmann, O. Yazyev, A.J. Austin, R. Cammi, C. Pomelli, J.W. Ochterski, P.Y. Ayala, K. Morokuma, G.A. Voth, P. Salvador, J.J. Dannenberg, V.G. Zakrzewski, S. Dapprich, A.D. Daniels, M.C. Strain, O. Farkas, D.K. Malick, A.D. Rabuck, K. Raghavachari, J.B. Foresman, J.V. Ortiz, Q. Cui, A.G. Baboul, S. Clifford, J. Cioslowski, B.B. Stefanov, G. Liu, A. Liashenko, P. Piskorz, I. Komaromi, R.L. Martin, D.J. Fox, T. Keith, M.A. Al-Laham, C.Y. Peng, A. Nanayakkara, M. Challacombe, P.M.W. Gill, B. Johnson, W. Chen, M.W. Wong, C. Gonzalez, J.A. Pople, Gaussian, Inc., Wallingford CT, 2004.
[20] J.S. Binkley, J.A. Pople, W.J. Hehre, J. Am. Chem. Soc. 102 (1980) 939.
[21] (a) T.H. Dunning, P.J. Hay, H.F. Schaefer, In Modern Theoretical Chemistry; third ed., vol. 3, Plenum Press, New York, 1976, p. 1;
(b) P.J. Hay, W.R. Wadt, J. Chem. Phys. 82 (1985) 299;
(c) P.J. Hay, W.R. Wadt, J. Chem. Phys. 82 (1985) 270.
[22] (a) F. London, J. Phys. Radium, Paris 8 (1937) 397;
(b) R. Mcweeny, Phys. Rev. 126 (1962) 1028;
(c) R. Ditchfield, Mol. Phys. 27 (1974) 789;
(d) J.L. Dodds, R. Mcweeny, A.J. Sadlej, Mol. Phys. 41 (1980) 1419;
(e) K. Wolniski, J.F. Hilton, P. Pulay, J. Am. Chem. Soc. 112 (1990) 8251.
[23] (a) R. Bauernschmitt, R. Ahlrichs, Chem. Phys. Lett. 256 (1996) 454;
(b) R.E. Stratmann, G.E. Scuseria, M.J. Frisch, J. Chem. Phys. 109 (1998) 8218;
(c) M.E. Casida, C. Jamorski, K.C. Casida, D.R. Salahub, J. Chem. Phys. 108 (1998) 4439.
[24] (a) V. Barone, M. Cossi, J. Phys. Chem. A 102 (1998) 1995;
(b) M. Cossi, V. Barone, J. Chem. Phys. 115 (2001) 4708;
(c) M. Cossi, N. Rega, G. Scalmani, V. Barone, J. Comput. Chem. 24 (2003) 669.
[25] V.N. Nemykin, P. Basu, VMOdes: a virtual molecular orbital description program for GAUSSIAN, GAMESS and HYPERCHEM, Revision A 7.1, Department of Chemistry, Duquesne University, Pittsburgh, PA, 2001/2003.